Effect of quenched impurities on long-range order in systems with a frustrated ground state

Y. Shnidman and D. Mukamel
Department of Physics, Weizmann Institute of Science, Rehovot, Israel
(Received 28 November 1983)

Destruction of long-range order (LRO) in interacting systems with a frustrated ground state due to quenched dilution is discussed. In such systems there is an additional contribution to the disordering process when initially frustrated bonds become satisfied as dilution removes the competing bonds. It is therefore expected that at $T=0$, LRO vanishes at an impurity concentration q_L which is lower than the corresponding percolation threshold impurity concentration q_c. To study this phenomenon the anisotropic Ising antiferromagnet on a triangular lattice with quenched site dilution is analyzed. An estimate for q_L is obtained by means of series-expansion methods. This model may describe the magnetic phase of oxygen adsorbed on graphite which has been of considerable interest in recent years.

I. INTRODUCTION

The effect of quenched impurities on the phase diagram of an interacting system is a frequently encountered experimental phenomenon. Many such systems may be represented by a magnetic spin model with short-range exchange interactions in which quenched nonmagnetic impurities are distributed homogeneously with some given concentration c. Consider a simple model in the "pure" ($c=0$) state which has an unfrustrated, ordered ground state at zero temperature and undergoes a second-order phase transition into a disordered phase at some critical temperature $T_c>0$. The simplest example is the ferromagnetic Ising model on any lattice of dimensionality d higher than $d=1$. Introduction of quenched impurities with homogeneous concentration c is modeled by allowing a probability q for any lattice site to be vacant and probability $p=1-q$ to be occupied by a spin, where $q \propto c$. Now consider the long-range order (LRO) in such a system, which exists for sufficiently low temperature T and concentration c. LRO in a pure, $c=0$ system is destroyed at $T=T_c$ due to thermal fluctuations in the spin system. On the other hand, at $T=0$ there are no thermal fluctuations at all, but nevertheless LRO is destroyed through a second-order phase transition at sufficiently high q. This order-disorder transition when increasing q at $T=0$ is induced by an increase in "geometric" disorder in the system. Finite clusters of magnetic ions cannot support LRO, but an infinite cluster is completely ordered at $T=0$ in nonfrustrated systems. Thus in such systems the order parameter (magnetization per lattice site) at $T=0$ is given by

$$m(p,T=0)=P_\infty(p)\ , \tag{1}$$

where P_∞ is the fraction of occupied sites belonging to the infinite percolating cluster. Note that $P_\infty(p)=pP(p)$, where $P(p)$ is the usual percolation probability.[1] This means that at $T=0$ the LRO is destroyed exactly at p_c, the percolation threshold for the corresponding site percolation problem on that lattice.[1]

For nonzero temperature the established picture for the phase diagram is as follows. The p-T plane is separated into ordered and disordered phases by a line of critical points connecting the "pure" Ising critical point at $p=1, T=T_c$ to the percolation critical point at $p=p_c, T=0$, as shown schematically by line a in Fig. 1. At finite T, the critical exponents are those of the Ising universality class. As one approaches the "multicritical" point[2] $p=p_c, T=0$ from above, there is a crossover to percolation critical exponents with crossover exponent $\phi=1$.

A most interesting question, both experimentally and theoretically, is how the p-T phase diagram is modified for systems which have a macroscopic fraction of *frustrated*[3] bonds in the ground state. Qualitatively, it is easy to see that two mechanisms contribute to the destruction of LRO at $T=0$ when quenched impurities are introduced into such a system. First, there is the effect of formation of disconnected finite clusters completely isolated from the infinite cluster by a perimeter of vacancies. The magnetization in those clusters is free to fluctuate, thus reduc-

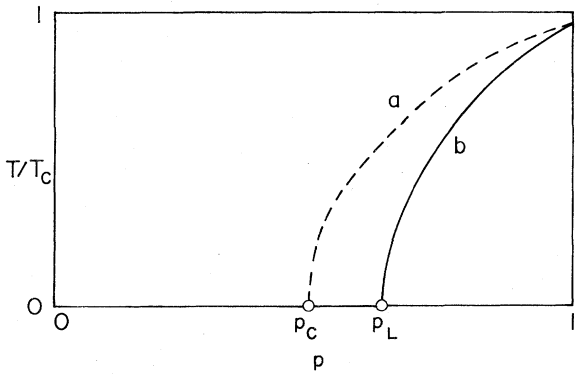

FIG. 1. Schematic p-T phase diagrams for Ising models with quenched site dilution for systems with (a) nonfrustrated and (b) frustrated ground states. Here p_c is the percolation threshold probability, and p_L is the site occupation probability below which there is no LRO at $T=0$ in the frustrated case.

 ©1984 The American Physical Society

ing the average magnetization per site. This is the origin of the "geometric" disorder also in the nonfrustrated systems. However, in a system with a *frustrated* ground state the average magnetization per site can also be reduced when a bond, which was initially frustrated in the undiluted system at $T=0$, is "relieved" of frustration as dilution removes the competing bonds. Thus, in systems with a frustrated ground state, geometric disorder induces a *decrease* in LRO. For such a system, Eq. (1) is not valid; the $T=0$ order parameter in those systems should be given instead by

$$m(p,T=0)=R(p)P_{\infty}(p)\ , \tag{2}$$

where for systems with a frustrated ground state, $R(p)<1$ at any p. It is reasonable to expect that at $T=0$ the LRO is destroyed at some critical probability $q_L=1-p_L$ which is *lower* than the percolation threshold $q_c=1-p_c$. In other words, when diluting such a system the LRO is destroyed *before* the probability for formation of an infinite cluster becomes zero. Hence, the p-T phase diagram should resemble line b for a system with a frustrated ground state, as compared with line a for a system with a nonfrustrated ground state (see Fig. 1).

We expect the phenomenon described above to occur in many experimental systems. Two explicit examples are considered in some detail in Sec. II. Both are $d=2$ systems of diatomic molecules adsorbed on graphite, diluted by inert-gas atoms. The frustrated ground states are the "herringbone" phase exhibited by the system of N_2 molecules adsorbed on graphite and the antiferromagnetic ϵ phase of O_2 molecules adsorbed on graphite.

In order to study the effect of quenched site impurities on the LRO in frustrated systems in a more quantitative fashion, we introduce a simple theoretical model in Sec. III. This is the anisotropic Ising nearest-neighbor antiferromagnetic model on a triangular lattice with quenched site dilution. The model is then studied quantitatively at $T=0$ using the series-expansion method for both high- and low-density limits, and an estimate for q_L is obtained. In Sec. IV we discuss the results of this study, list several related phenomena, and state some open questions about the type of critical behavior of this class of systems.

II. EXPERIMENTAL SYSTEMS

Here we present two explicit examples of experimental systems with frustrated ground states which should behave in the manner described in the preceding section. First, consider the system of N_2 molecules adsorbed on graphite. At coverages equal or below $\frac{1}{3}$ and at sufficiently low temperatures the molecules form a $(\sqrt{3}\times\sqrt{3})30°$ commensurate structure in registry with the hexagonal lattice of the substrate.[4] Upon further lowering of temperature, the system undergoes a phase transition from a phase in which the molecular axes are randomly oriented to a phase in which they are orientationally ordered. Low-energy electron-diffraction measurements[5] have led to the identification of the low-temperature phase as a (2×1) herringbone structure of oriented molecules. The ground state is sixfold degenerate. One of those six equivalent ground-state orderings is shown schematically in Fig. 2(a). This structure arises due to the anisotropic interactions of N_2 molecules with the substrate and with each other. The N_2-substrate interaction tends to orient the molecular axes in the plane of the graphite.[6] Since the N_2 molecules possess a relatively large electric quadrupole moment, the intermolecular N_2-N_2 interaction is well described by the electric quadrupole-quadrupole (EQQ) interaction.[7] The EQQ interaction favors pairs of N_2 molecules to be oriented perpendicularly to each other. Thus we see that in the herringbone structure shown in Fig. 2(a) every horizontal bond is frustrated.

A second example is provided by the system of O_2 molecules adsorbed on graphite. The coverage-temperature (ρ'-T) phase diagram has been under intensive experimental study in recent yeaars.[8] The O_2 molecule is anisotropic with an egg-shaped form, and has a spin $S=1$. The magnetic moment of O_2 is oriented perpendicularly to the molecular axis. At sufficiently high coverages and low temperatures, the molecular axes of O_2 molecules are oriented perpendicular to the substrate plane, and form an equilateral (distorted) triangular lattice.[9] Neutron-diffraction studies[10] show that the ground state is antiferromagnetic, with the molecular magnetic moments being parallel to the substrate plane and forming a two-sublattice collinear structure as shown in Fig. 2(b). This low-temperature, two-dimensional antiferromagnetic phase is referred to as the ϵ phase[8] in the literature, and it has the same structure as the basal plane of the antiferromagnetic α phase[11] of bulk solid O_2. The dominant interaction between a pair of O_2 molecules is the antiferromagnetic exchange interaction. Assuming only the four nearest-neighbor and the two next-nearest-neighbors interactions to be important, Bhandari and Falicov[12(a)] estimated $|J_1|=0.005$ eV for the nearest-neighbor exchange constants and $|J_2|=0.003$ eV for the second-nearest-neighbor exchange constants. More recent *ab initio* calculations[12(b)] by Van Hemet *et al.* yield $J_2/J_1=0.42$. Thus we see that in the antiferromagnetic ground state shown in Fig. 2(b) every horizontal bond is frustrated. Recently, specific-heat measurements[13] established that as temperature is increased, the system undergoes a phase transition from the antiferromagnetic phase to a paramagnetic phase, with the *same distorted triangular* arrangement. Those measurements also indicate that this transition belongs to the Ising universality class.[13,14]

In principle, both experimental systems described above

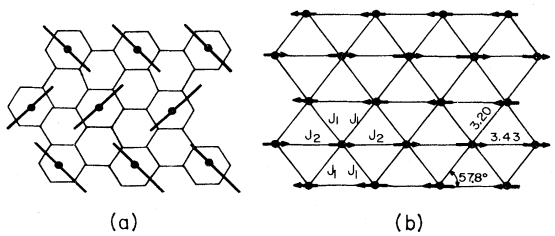

FIG. 2. (a) One of the sixfold-degenerate ground states corresponding to the herringbone phase of N_2 molecules adsorbed on graphite. (b) One of the twofold-degenerate antiferromagnetic ground states corresponding to the ϵ phase of O_2 molecules adsorbed on graphite.

can be diluted by inert-gas impurities. For example, ^{4}Ar or Kr atoms can be used to dilute the N_2-on-graphite herringbone structure, and ^{4}He atoms can be used to dilute the O_2-on-graphite antiferromagnetic structure. However, it may be nontrivial experimental problem to perform the dilution homogeneously and in a quenched manner.

In order to study the effect of quenched impurities on LRO in systems such as N_2 and O_2 on graphite, we have to approximate those systems by a simple theoretical model. We found it easier to do it for the case of O_4 on graphite. Nevertheless, we expect that the same *qualitative* features should also characterize the N_2-on-graphite system.

III. THEORETICAL MODEL: SERIES-EXPANSION APPROACH

In this section we introduce a simple theoretical model which may describe the O_2-on-graphite system in the regime of the antiferromagnetic-to-paramagnetic phase transition. As such, we choose the nearest-neighbor Ising model on the triangular lattice with anisotropic exchange constants

$$H=-\tfrac{1}{2}\sum_{n,m}[J_1(S_{n,m}S_{n+1,m}+S_{n,m}S_{n+1,m+1}) +J_2(S_{n,m}S_{n,m+1})] , \tag{3}$$

such that $|J_1| \gg |J_2|$, and $J_1<0$ and $J_2<0$. The ground state of this model, which is a (2×1) structure, consists of ferromagnetic horizontal rows coupled antiferromagnetically (see Fig. 3). This is the same structure found in the ϵ phase of O_2 on graphite [Fig. 2(b)]. It is useful to note that the Hamiltonian (3) is invariant under the transformation $J_1\rightarrow -J_1$, and $S_{n,m}\rightarrow\sigma_{n,m}=(-1)^m S_{n,m}$. The ground state of this Hamiltonian in the σ variables is ferromagnetic. Thus the destruction of LRO is signaled by the vanishing of the magnetization and a singularity in the susceptibility. The same is true for staggered magnetization and staggered susceptibility when the S variables are used. The undiluted model described here undergoes a second-order phase transition belonging to the Ising universality class at the critical temperature T_c given by[15]

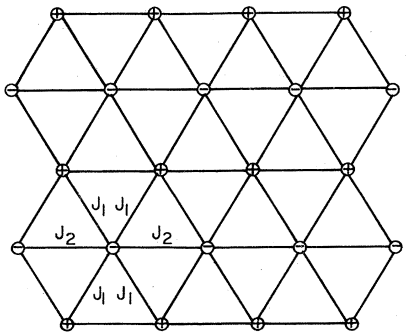

FIG. 3. One of the two degenerate ground states corresponding to the anisotropic Ising antiferromagnet on the triangular lattice ($J_1<0$, $J_2<0$, and $|J_2|/|J_1| \ll 1$).

$$\sinh^2(2J_1/k_BT)+2\sinh(2J_1/k_BT_c)\sinh(2J_2/k_BT_c)=1 . \tag{4}$$

Let us now introduce quenched site dilution with equal probability p for any site to be occupied. To estimate the probability at which the LRO is destroyed at $T=0$ (which will be denoted by p_L, to avoid confusion with the percolation critical probability p_c), we used series-expansion techniques. In the high-density limit, the first terms in the series expansion of the magnetization in powers of q, for small q, were obtained. In the low-density limit the first terms in the series expansion of the susceptibility in powers of p, for small p, were found. We wish to emphasize that, in general, p_L may depend on the ratio $|J_2|/|J_1|$, since different values of this ratio lead to different series. In the present work we assumed that J_2/J_1 is infinitesimal, but nonzero. Note that for the case $J_1>0$ and $J_2=0$, $p_L=p_c^{\rm sq}$, but for any $J_2>0$ (even if it is infinitestimal) we have $p_L=p_c^{\rm tr}$. Here $p_c^{\rm sq}=0.593$ (Ref. 16) and $p_c^{\rm tr}=\frac{1}{2}$ (Ref. 17) are the site percolation probabilities for the square and triangular lattices, respectively. Let us now briefly describe the methods used in deriving the series expansions.

A. High-density magnetization

Our method for derivation of the series for magnetization at $T=0$ in the high-density limit is similar to the method used by Grinstein *et al.*[18] for quenched random Ising magnets with mixed nearest-neighbor couplings J. The derivation of the series in the ferromagnetic phase is based on a decomposition $\mathscr{D}$ into graphs of vacancies which contribute additively to the decrease of total magnetization per site. Thus

$$\overline{m}=1-\sum_{G\in\mathscr{D}}\Delta M(G)P(G) , \tag{5}$$

where $\overline{m}$ is the quenched average magnetization per site, and ΔM is the reduction in $M=\sum_i m_i$ from the full lattice value $M=N$ due to a single graph G, m_i being the magnetization at site i and N being the total number of sites in the lattice. Here $P(G)$ is the conditional probability per lattice site of finding the graph G, provided that this graph is not a subgraph of any higher-order graph that belongs to the decomposition $\mathscr{D}$.

If G contains n vacancies, then $P(G)$ is an infinite series in powers of q, whose lowest-order term is proportional to q^n. We have carried the series expansion of $\overline{m}$ to order q^7. Figure 4 shows all the graphs to that order, and Table I lists the corresponding calculated values of $P(G)$ (to order q^7) and $M(G)$. Our calculation suffers from the same complication as the calculation by Grinstein *et al.*[18] Namely, the decomposition into additively contributing graphs of vacancies cannot be reduced to connected graphs only. Thus the connected components in the graphs (b), (d)—(h), and (k) (Fig. 4) do not contribute additively to M. This is because in those graphs the disconnected clusters of vacancies, when all of them are present, remove all the dominant bonds. Hence, initially frustrat-

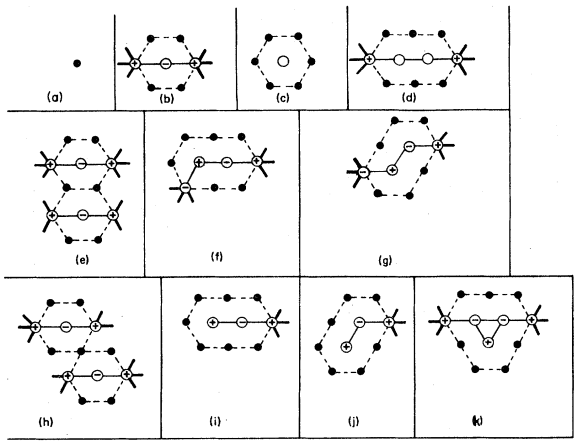

FIG. 4. All of the graphs used in calculating the high-density series, expansion of $\overline{m}(q)$ to order q^7. Solid circles denote vacant sites, and open circle with fixed sign denote spins of fixed sign. Open circles in (c) is not labeled by sign since it can be $(+)$ or $(-)$ with equal probability of $\frac{1}{2}$. Similarly, the pair of open circles in (d) stands for this pair of spins being $(+,-)$, $(-,+)$, or $(-,-)$ with equal probability of $\frac{1}{3}$. Thin solid lines denote bonds which are free to flip to minimize the energy of the graph. Thick solid lines denote bonds which are fixed (frustrated or nonfrustrated) as in the ground state. The dashed lines serve merely as a guide to the eye.

ed bonds become satisfied, leading to the flipping of spins and thus contributing to M. This contribution is nonadditive, since when only one component is present, not all dominant bonds are removed, and hence the initially frustrated bonds remain frustrated. This phenomenon is characteristic of systems with a frustrated ground state. When the ground state is nonfrustrated, the decomposition into additively contributing graphs of vacancies can be reduced to connected graphs only.

The necessity to consider disconnected graphs has severely limited the length of the series that were able to obtain. We are not aware of any convenient algorithm for identifying all graphs entering to given order in q. Thus we are able to carry the expansion only to order q^7, and the result is

TABLE I. Occurrence probabilities and magnetization reductions for the graphs of Fig. 1.

Graph	$\Delta M(G)$	$P(G)$ to order q^7
(a)	1	$q(1-4q^3+4q^4-30q^5-58q^6)$
(b)	6	$q^4(1-q-9q^2+9q^3)$
(c)	7	$q^6(1-q)$
(d)	$\frac{26}{3}$	$q^6(1-4q)$
(e)	10	$q^6(1-2q)$
(f)	8	$4q^6(1-4q)$
(g)	10	$4q^6(1-4q)$
(h)	11	$2q^7$
(i)	9	$6q^7$
(j)	11	$4q^7$
(k)	13	$4q^7$

$$\overline{m}(q)=1-q-2q^4+2q^5-\tfrac{41}{3}q^6+\tfrac{35}{3}q^7+\cdots . \quad (6)$$

For comparison, the first terms in the series expansion of the $T=0$ magnetization $m(q)$ for the nonfrustrated site-diluted ferromagnet on a triangular lattice are

$$m(q)=1-q-q^6+q^7-6q^8+6q^9+\cdots . \quad (7)$$

Note that the first nontrivial contribution to m is of the order q^4, as compared with q^6 in the nonfrustrated case. This agrees with the qualitative arguments presented before, that the magnetization of the frustrated model should decay faster than that of the nonfrustrated model as one increases the concentration of impurities. In Fig 5(a) the order parameter $\overline{m}(q)$ is plotted to orders 4, 5, 6, and 7, as well as the [3,3] Padé approximant to $\overline{m}(q)$. For comparison, in Fig. 5(b) the $T=0$ magnetization $m(q)$ for the nonfrustrated site-diluted ferromagnet on a triangular lattice is plotted to orders 6, 7, 8, and 9, as well as the [3,5] Padé approximant for $m(q)$.

We have applied the standard log-derivative Padé analysis[19] to the series (6). Thus we have found the poles on the real axis and the corresponding residues for the Padé approximants to $d\ln\overline{m}(q)/dq$. The results are shown in Table II. We see that the series is dominated by a nonphysical singularity at $q\simeq-0.28$ with residue having a value which approximately equals 0.02. This is similar to the ordinary site percolation, where the series for $P(q)$ is also dominated by a nonphysical singularity on the negative real axis. In Table II there is also a physi-

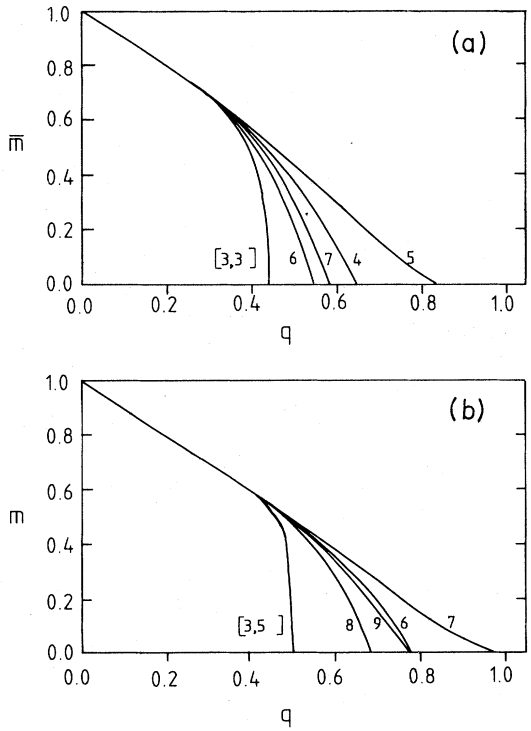

FIG. 5. (a) Plots of $\overline{m}(q)$, where $\overline{m}(q)$ is given by (6), to orders 4, 5, 6, and 7 in q. The [3,3] Padé approximant to $m(q)$ is also shown. (b) Plots of $m(q)$, where $m(q)$ is given by (7), to orders 6, 7, 8, and 9 in q. The [3,5] Padé approximant to $m(q)$ is also shown.

TABLE II. Real-axis poles and residues of the Padé approximants to $d\ln\overline{m}(q)/dq$, where $\overline{m}(q)$ is given by (6).

	$q>0$		$q<0$	
Approximant	Pole	Residue	Pole	Residue
[2,2]	0.3702	0.1006	−0.2702	0.0194
[3,2]	0.3808	0.1125	−0.2816	0.0233
[2,3]	0.3805	0.1118	−0.2819	0.0232
[3,3][a]	0.3627	0.0964	−0.2742	0.0204

[a]For [3,3] there is also a spurious pole at $q=0.1586$.

cal singularity on the positive real axis, and the pole-residue plot for it is given in Fig. 6. The close consistency of the Padé approximants shown in Table II suggest that the destruction of LRO occurs by means of a second-order transition characterized by $p_L \simeq 0.63$ and $\beta_L \simeq 0.1$. We therefore find that $p_L > p_c^{\rm tr}$. However, due to the fact that the series is rather short, our result does not exclude the possibility that in the limit $J_2/J_2 \ll 1$, $p_L = p_c^{\rm sq}$.

B. Low-density susceptibility

In order to calculate the first terms in the low-density expansion for the susceptibility at $T=0$, we used the identity

$$\chi_0(p) = \lim_{T\to 0} k_B T \chi(T,p) = \sum_G M^2(G) P(G) , \tag{8}$$

where the summation is over all finite isolated clusters G of occupied sites, $M(G)$ is the magnetization of the cluster, and $P(G)$ is the probability per site to find this cluster on the lattice. Now, in the case of a dilute nonfrustrated magnet, the magnetization of a cluster containing s sites is $M=\pm s$, and therefore (8) can be rewritten as

$$\chi_0(p) = \sum_s s^2 n_s(p) = \sum_s s^2 p^s D_s(q) , \tag{9}$$

where $n_s(p)$ is the probability per site to find a cluster of size s, and $D_s(q)$ is the so-called perimeter polynomial.[1] In our case it is no longer true that $M=\pm s$; this is due to the effect of bonds, initially frustrated in the ground state, but which now turn out to be satisfied due to the absence of dominant bonds. In general, the energy of every finite cluster should be minimized to find the magnetization of that cluster. One such cluster with corresponding degenerate magnetizations and occurrence probability is shown in Fig. 7. In any case, M is an integer, such that $-s \le M \le s$. Thus, instead of (9) we can use

$$\chi_0(p) = \sum_s \sum_{M^2\le s^2} M_s^2 n_{s,M}(p) = \sum_s p^s \sum_{M^2\le s^2} M_s^2 D_{s,M}(q) , \tag{10}$$

where $n_{s,M}$ is the probability per site to find a cluster of size s, and the value of magnetization squared M^2, and $D_{s,M}(q)$ is the corresponding modified perimeter polynomial. Thus the only change in the algorithm as compared to the ordinary percolation case is the decomposition of cluster classes of a given size into subclasses according to their value of magnetization squared, which is found by energy minimization.

Considering clusters of size less than or equal to $s=6$, we have constructed the modified perimeter polynomials and derived the first terms up to order p^6 manually. The corresponding modified perimeter polynomials are given in Table III. The resulting series expansion to order p^6 for (p) is

$$\chi_0(p) = p + 2p^2 + 10p^3 + 8p^4 + 30p^5 + 32p^6 + \cdots , \tag{11}$$

Unfortunately, the series is not sufficiently long to produce a sensible result when subjected to the standard ratio and log-derivative Padé analysis. At first glance this is somewhat surprising since, for example, a series expansion of comparable order for the dilute nonfrustrated ferromagnet on a triangular lattice gives a reasonable estimate for p_c,[20] as compared to the exact value of $p_c = \frac{1}{2}$.[17] However, we see in (11) a "pairing" effect between odd and even terms in the expansion. This is probably due to the existence of nonfrustrated antiferromagnetic bonds in the clusters. As a result, series of double length are neces-

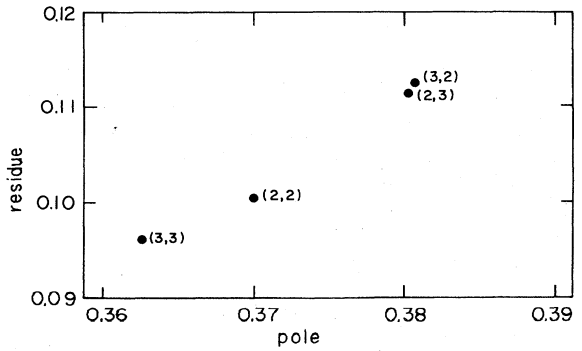

FIG. 6. Pole-residue plot for the singularities on the positive real axis of the Padé approximants of $d\ln\overline{m}(q)/dq$.

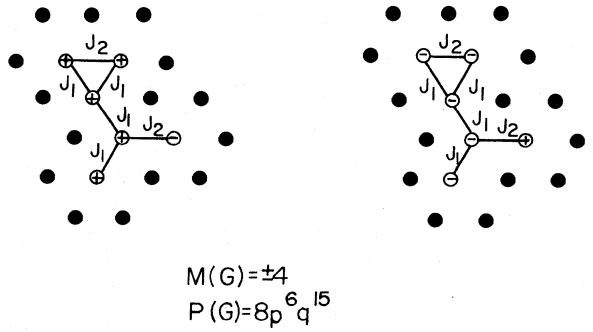

FIG. 7. Example of one of the finite clusters used in calculating the low-density series expansion for the susceptibility. Open circles denote spins belonging to the finite cluster with their corresponding signs. Solid circles denote vacant perimeter sites, and bonds are denoted by lines.

TABLE III. List of modified perimeter poynomials $D_{s,M}$ for clusters of size less than 7, used in derivation of the low-density expansion for the susceptibility [Eq. (17)]. Note that $\sum_M D_{s,M}=D_s$, where D_s is the ordinary perimeter polynomial for clusters of size s in the site percolation problem on the triangular lattice.

$D_{1,1}=q^6$
$D_{2,2}=2q^8$, $D_{2,0}=q^8$
$D_{3,3}=2q^9+4q^{10}$, $D_{3,1}=5q^{10}$
$D_{4,4}=3q^{10}+8q^{11}+8q^{12}$, $D_{4,2}=4q^{11}+14q^{12}$, $D_{4,0}=7q^{12}$
$D_{5,5}=6q^{11}+15q^{12}+26q^{13}+16q^{14}$, $D_{5,3}=6q^{12}+24q^{13}+38q^{14}$, $D_{5,1}=16q^{13}+39q^{14}$
$D_{6,6}=14q^{12}+30q^{13}+68q^{14}+72q^{15}+32q^{16}$, $D_{6,4}=12q^{13}+50q^{14}+100q^{15}+100q^{16}$
$D_{6,2}=27q^{14}+84q^{15}+118q^{16}$, $D_{6,0}=q^{13}+8q^{14}+42q^{15}+56q^{16}$

sary in our case in order to obtain results of comparable accuracy with the $\chi_0(p)$ series of the dilute nonfrustrated ferromagnet.

We obtained better results from the high-density expansion than from the low-density expansion; however, the low-density expansion is potentially more promising since it is suitable for programming on a computer. We see that a convenient algorithm exists for calculation of the low-density susceptibility (which is not the case for the high-density magnetization). However, as in usual percolation, the number of clusters grows exponentially with size,[21] and, moreover, the energy of each cluster should be minimized in order to find the magnetization. Thus one has to resort to the computer in order to obtain long series, and even then there is a severe constraint due to computation time.

IV. DISCUSSION

In this paper we studied the anisotropic Ising model on a triangular lattice with quenched site dilution. This model has a frustrated ground state in the undiluted case. A series expansion in the high-density limit indicates that in such a system the order parameter vanishes at a lower impurity concentration than the corresponding percolation threshold impurity concentration. The series expansion for the susceptibility in the low-density limit is inconclusive to the order that we were able to obtain manually; however, we believe that our algorithm can be programmed for use on a computer and can thus provide results to much higher orders.

The theoretical model that we studied may describe the dilution of the magnetic phase of O_2 adsorbed on graphite by nonmagnetic impurities, provided that a more realistic value for $|J_2|/|J_1|$ (e.g., that of Ref. 12) is put into the numerical calculations. However, this will be true only if the dilution in the real system were of the quenched, not annealed, type. Also, it is not clear whether neglecting the interaction between the impurities themselves is justified; if not, the probability for a given site to be occupied by an impurity is not independent of that probability on other sites, as in the case of correlated percolation. Finally, in studying specific experimental systems one should not exclude *a priori* the possibility of an intermediate phase characterized by a different order parameter due to competition between the dominant and frustrated bonds and the disorder due to dilution.

We believe that many experimental systems should exhibit the qualitative behavior described in this paper. The magnetic system of diluted O_2 adsorbed on graphite is but one example for which we found a simple theoretical model. Another example which has been provided in this paper is the diluted herringbone phase of N_2 adsorbed on graphite. Both examples are two dimensional, but the same qualitative phenomena could occur also in three-dimensional systems with a frustrated ground state.

From the theoretical point of view, the same qualitative behavior should characterize systems with quenched bond dilution as systems with quenched site dilution, which we considered here. Also, it will be instructive to compare phase diagrams of systems with annealed vacancies having frustrated and nonfrustrated ground states.

An important question which is left unanswered by this study concerns the type of critical behavior exhibited by the systems of the kind described above at the $T=0$ order-disorder transition. We have seen that the impurity concentration at which it happens is lower than the corresponding percolation threshold impurity concentration. The question is whether or not the transition belongs to a universality class which is different from that of the percolation phase transition. Our estimates for the exponent β_L, given by the residues of the physical poles in Table II, were not sufficiently accurate to give a decisive answer to this question. We hope to address this problem in a future study using more accurate numerical methods. Another subject for a future study is exploration of the p-T phase diagram at nonzero temperature.

Note added in proof. Recently, the phase diagram of argon-diluted nitrogen films adsorbed on graphite has been studied [A. D. Migone, Zhong-song Li, M. H. W. Chan, and M. R. Gini, Phys. Rev. B 28, 6525 (1983)] using high-resolution heat-capacity techniques. According to this study, the transition temperature $T_c(p)$ is significantly depressed by the Ar impurities. Extrapolation of $T_c(p)$ to zero temperature indicates that at $T=0$, LRO is destroyed at $p=p_c$, where $p_L>p_c^{\rm tr}$. The frustration mechanism, discussed in this paper, may explain this experimental result.

ACKNOWLEDGMENTS

We thank L. Passell and S. Satija for illuminating discussions on the phase diagram of N_2 on graphite which initiated this study. We also thank A. Aharony, E. Domany, C. Domb, and S. Fishman for helpful discussions. This work was supported in part by a grant from the Israel Academy of Sciences and Humanities, Basic Research Foundation.

[1]J. W. Essam, Rep. Prog. Phys. 43, 833 (1980).
[2]D. Stauffer, Z. Phys. B 22, 161 (1975); T. C. Lubensky, Phys. Rev. B 15, 311 (1975); A. Coniglio, Phys. Rev. Lett. 46, 250 (1981).
[3]G. Toulouse, Common. Math Phys. 2, 115 (1977); J. Vannimenus and G. Toulouse, J. Phys. C 10, L537 (1977); G. Toulouse, J. Vannimenus, and J. M. Maillard, J. Phys. Lett. 38, L459 (1977).
[4]J. K. Kjems, L. Passell, H. Taub, and J. G. Dash, Phys. Rev. Lett. 32, 724 (1974); J. K. Kjems, L. Passell, H. Taub, J. G. Dash, and A. D. Novaco, Phys. Rev. B 13, 1466 (1976).
[5]R. D. Diehl, M. F. Toney, and S. C. Fain, Jr., Phys. Rev. Lett. 43, 1329 (1979).
[6]W. A. Steel, J. Phys. (Paris) Colloq. 38, C4-61 (1977).
[7]T. A. Scott, Phys. Rep. 27, 89 (1976).
[8]For a recent phase diagram of O_2 adsorbed on graphite, see D. D. Awschalom, G. N. Lewis, and S. Gregory, Phys. Rev. Lett. 51, 586 (1983). However, according to Ref. 13, ζ denotes not one, but two paramagnetic phases.
[9]P. A. Heiney, P. W. Stephens, S. G. I. Mochrie, I. Akimitsu, and R. I. Birgeneau, Surf. Sci. 125, 539 (1983).
[10]J. P. McTague and M. Nielsen, Phys. Rev. Lett. 37, 596 (1976); M. Nielsen and J. P. McTague, Phys. Rev. B 19, 3096 (1979).
[11]M. F. Collins, Proc. Phys. Soc. London 39, 415 (1966); C. S. Barrett, L. Meyer, and J. Wasserman, J. Chem. Phys. 47, 592 (1967).
[12](a) R. Bhandari and L. M. Falicov, J. Phys. C 6, 479 (1973); (b) M. C. Van Hemet, P.E.S. Wormer, and A. van der Avoind, Phys. Rev. Lett. 51, 1167 (1983).
[13]R. Marks and B. Christoffer, Phys. Rev. Lett. 51, 790 (1983).
[14]Universality class and critical properties of the described phase transition were examined theoretically by E. Domany and E. K. Reidel, Phys. Rev. B 19, 5817 (1979).
[15]R. M. F. Houtappel, Physica 16, 426 (1950).
[16]P. J. Reynolds, H. E. Stanley, and W. Klein, Phys. Rev. B 21, 1223 (1980).
[17]M. F. Sykes and J. W. Essam, J. Math. Phys. 5, 1117 (1964).
[18]G. Grinstein, C. Jayaprakash, and M. Wortis, Phys. Rev. B 19, 260 (1979).
[19]D. S. Gaunt and A. J. Guttmann, in *Phase Transitions and Critical Phenomena,* edited by C. Domb and M. S. Green, (Academic, New York, 1974), Vol. 3, Chap. 4.
[20]This can be seen by ratio analysis of the low-density series expansion for mean cluster size in the site percolation problem, given in Ref. 21 and truncated to order 6 in cluster size.
[21]M. F. Sykes and M. Glen, J. Phys. A 9, 87 (1976).